JCTC Journal of Chemical Theory and Computation

Article

pubs.acs.org/JCTC

Ionization Energies, Electron Affinities, and Polarization Energies of Organic Molecular Crystals: Quantitative Estimations from a Polarizable Continuum Model (PCM)-Tuned Range-Separated Density Functional Approach

Haitao Sun,[†,‡] Sean Ryno,[†] Cheng Zhong,[†] Mahesh Kumar Ravva,[†] Zhenrong Sun,[‡] Thomas Körzdörfer,[*,§] and Jean-Luc Brédas[*,†]

[†]Solar & Photovoltaics Engineering Research Center, Physical Science and Engineering Division, King Abdullah University of Science and Technology (KAUST), Thuwal 23955-6900, Kingdom of Saudi Arabia

[‡]State Key Laboratory of Precision Spectroscopy, School of Physics and Materials Science, East China Normal University (ECNU), Shanghai 200062, People's Republic of China

[§]Institut für Chemie, Universität Potsdam, Potsdam 14476, Germany

Supporting Information

ABSTRACT: We propose a new methodology for the first-principles description of the electronic properties relevant for charge transport in organic molecular crystals. This methodology, which is based on the combination of a nonempirical, optimally tuned range-separated hybrid functional with the polarizable continuum model, is applied to a series of eight representative molecular semiconductor crystals. We show that it provides ionization energies, electron affinities, and transport gaps in very good agreement with experimental values, as well as with the results of many-body perturbation theory within the GW approximation at a fraction of the computational costs. Hence, this approach represents an easily applicable and computationally efficient tool to estimate the gas-to-crystal phase shifts of the frontier-orbital quasiparticle energies in organic electronic materials.

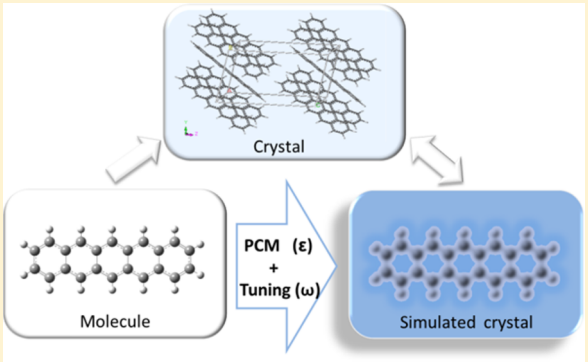

1. INTRODUCTION

Organic semiconductors have attracted considerable interest because of their applications in new generations of plastic electronic and optoelectronic devices.[1−4] Design of novel materials requires a fundamental understanding of various phenomena such as photoexcitation, charge mobility, intra-molecular/intermolecular interactions, and solid-state polarizations (gap renormalization). In particular, the prediction of reliable quasiparticle energies and transport (fundamental) gaps is critical to understand mechanisms such as carrier injection and transport.[4,5] The solid-state transport gap (E_g) is defined as the minimum energy of formation of a pair of separated free electron and hole, that is, the difference between the ionization energy (IE) and electron affinity (EA).[6] Experimentally, these quantities can be determined via ultraviolet photoelectron spectroscopy (UPS) and inverse photoemission spectroscopy (IPES), respectively.[5]

From a theoretical standpoint, a particular challenge arises from the fact that the comparison between calculated quasiparticle energies at the single-molecule level and experimental measurements on crystals or thin films is by no means straightforward. In practice, it is found that the gas-phase molecular orbital energies evaluated from density functional theory (DFT) often agree quite well with the solid-state IE and EA experimental estimates, despite the fact that the former obviously do not account for solid-state effects.[7,8] A similarly fortuitous agreement is also often obtained when using the DFT frontier orbital energy gaps to represent the optical gaps measured with UV-vis spectroscopy, even though the exciton binding energies and excited-state correlation effects are completely ignored.[9,10] However, since such agreements are based on an uncontrolled cancellation of errors, the theoretical insights and predictions that can be obtained from gas-phase calculations are severely limited.

In addition to these theoretical challenges, the reported experimental data can sometimes vary significantly among measurements carried out by different research groups. As a consequence, the physical interpretation of these measurements can remain controversial.[11] To take a recent example involving two widely studied organic semiconductors, the IE of the pentacene crystal has been measured by the Lichtenberger

Received: February 29, 2016
Published: May 16, 2016

DOI: 10.1021/acs.jctc.6b00225
J. Chem. Theory Comput. 2016, 12, 2906−2916

group to be 4.81 eV,[12,13] which is 0.24 eV smaller than the IE measured by the Kahn group (5.05 eV);[14,15] on the other hand, the IE of tri-isopropylsilyl-ethynyl (TIPS)−pentacene determined by the Lichtenberger group (5.84 eV)[12,13] is 0.80 eV larger than that reported by the Kahn group (5.04 eV).[14,15] As a result, the solid-state polarization energies estimated for the TIPS-pentacene films are remarkably different: 0.44 eV by the Lichtenberger group vs 1.24 eV by the Kahn group.[16] Generally speaking, several factors can contribute to such significant variations between experimentally determined values,[16−19] such as (i) different ways to analyze the measurements, e.g., using peak onset or peak maximum values, and vertical or adiabatic values; (ii) morphology and degree of crystallinity of the molecular films; (iii) nature of the material surfaces, given the extreme surface sensitivity of UPS/IPES measurements; (iv) different substrates such as Au, Ag, SiO_2, or ITO and, related to that, different orientations of the molecules on the surface;[19] (v) uncontrolled environmental effects, temperature effects, and/or oxidation of the crystal/film surface; and (vi) resolution of the instruments and the general experimental setup. A reliable and computationally efficient method for the prediction of solid-state IEs, EAs, and transport gaps from first-principles would thus be highly beneficial, as it would allow one to assess the intrinsic materials properties and possibly help in determining the origin of variations in experimental results.

The "state-of-the-art" for the prediction of IEs, EAs, and transport gaps from first-principles is many-body perturbation theory within the GW approximation.[20] This method has been shown to provide quantitative predictions for the quasiparticle (QP) spectrum of organic and inorganic systems.[18,21−24] However, not only is GW computationally much more demanding than DFT, the fact that it is typically employed non-self-consistently also leads to a significant starting-point dependence.[25−31] For the case of the pentacene molecule, for example, it has been found that non-self-consistent G_0W_0 calculations based on a (semi)local DFT starting point underestimate the fundamental gap E_g in the gas phase by as much as 0.7 eV, while E_g calculated at the same level of theory for the pentacene crystal is found to be in good agreement with the experimentally determined solid-state E_g, likely due to a fortuitous cancellation of errors.[18] The G_0W_0 accuracy can be significantly improved by the introduction of self-consistency at the level of eigenvalues[26,32] or using "better" DFT starting points, such as the global hybrid PBE0[27,28,33] and short-range hybrid Heyd-Scuseria-Ernzerhof (HSE) functionals,[18] as well as standard[33] and nonempirically tuned long-range corrected hybrid functionals.[30,34] However, the application of hybrid functionals for periodic systems is still computationally demanding, in particular when using the large basis sets required to converge a G_0W_0 calculation.

A computationally less demanding method to determine the ground-state electronic structures of molecules and solids is DFT. Unfortunately, conventional (semi)local exchange-correlation (XC) functionals may fail completely in predicting the electronic structure in "difficult" cases, such as organic mixed-valence or donor−acceptor systems.[35−37] In molecular crystals, the surrounding environment is substantially different from that of isolated molecules due to polarization effects.[17] Polarization is essentially a phenomenon related to nonlocal correlation, which cannot be captured by semilocal XC functionals. Furthermore, as a consequence of the lack of derivative discontinuity,[38−40] as well as the large electron delocalization error[36,41] or self-interaction error[35,42,43] of conventional XC functionals, the calculated orbital energies of the highest occupied molecular orbital (HOMO) and the lowest unoccupied molecular orbital (LUMO) obtained from standard XC functionals do not correspond to the IE and EA, respectively. Semilocal XC functionals, for example, typically overestimate the HOMO level and underestimate the LUMO level, resulting in an eigenvalue gap (or transport gap) that is too small.[8,9,39] Range-separated functionals[44−47] satisfying the correct asymptotic behavior in the long-range limit were developed to address this issue (among others). However, the standard implementation of those functionals, which makes use of a fixed, empirical range-separation parameter, often overestimates HOMO−LUMO gaps for large π-conjugated systems and typically has a tendency to show too much Hartree−Fock (HF)-like character.[9,35,48,49]

To allow for an improved description of the frontier orbital energies obtained from long-range corrected hybrid functionals, the concept of an "optimal tuning" of the range-separation parameter (ω) was introduced.[50,51] This tuning procedure is based on the ionization potential (IP) theorem, which states that the negative HOMO energy ($-\varepsilon_H$) in exact Kohn−Sham DFT is equal to the vertical IE, that is, the difference in total energy between the neutral and cationic systems for a fixed geometry.[52] It has been demonstrated that the tuning concept yields reliable descriptions of both ground-state properties[35,52−55] and excited-state properties[9,56−58] of organic molecules and polymer chains.[48] The IP-tuning procedure has also been shown to predict frontier orbital energies of molecules with an accuracy comparable to the GW approximation at lower computational costs.[30,34,52,59] However, the IP-tuning concept cannot be straightforwardly applied to periodic systems such as organic crystals for two reasons. First, the tuning procedure requires the calculation of the total energy of the cationic system, which in periodic systems can only be achieved by introducing a background charge. Second, it has been proven that, when periodic boundary conditions are applied, all exchange-correlation functionals obey the IP theorem, despite the fact that their HOMO eigenvalues differ.[60,61] As a consequence, all range-separation parameters in long-range-corrected hybrid functionals also obey the IP theorem, and the tuning procedure is no longer applicable.

Hence, to benefit from the success of the IP-tuning concept also for the description of molecular crystals, alternative approaches must be investigated. Here, we introduce an approach that combines the IP-tuning concept with dielectric continuum theory, such as the polarizable continuum model (PCM).[62] Several reports have underlined that using such solvation models provides for a powerful and efficient strategy to simulate the impact of solid-state effects on molecular properties and processes.[8,63] For instance, Lipparini and Mennucci have successfully used the PCM model to determine the electronic coupling parameters in organic molecular crystals.[64] Several other recent studies have attempted to use a "functional optimization" concept toward the reliable prediction of band gaps in organic molecular crystals via the introduction of a magnitude-equivalent dielectric constant of the crystal. Skone et al. presented a self-consistent scheme for determining the optimal fraction of exact exchange (α) in the global hybrid functional PBEh via the inverse macroscopic dielectric function ($1/\varepsilon$).[65] Although this PBEh functional with an adjusted α parameter can reproduce reasonable solid-state gaps, gas-phase gaps and the solid-state polarization energy are not described as well.[17] Refaely-Abramson et al. proposed a

DOI: 10.1021/acs.jctc.6b00225
J. Chem. Theory Comput. 2016, 12, 2906−2916

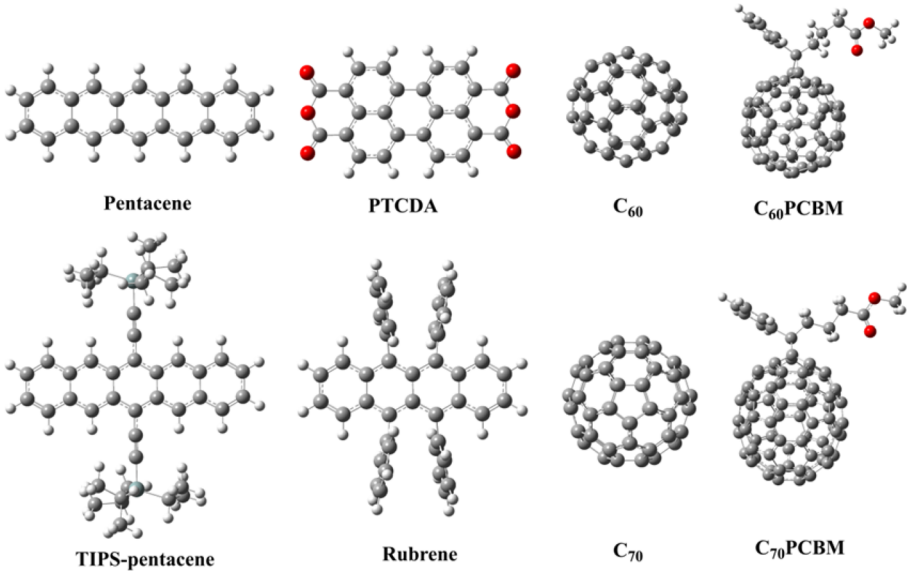

Figure 1. Molecular structures of pentacene, TIPS−pentacene, rubrene, PTCDA, C_{60}, C_{70}, C_{60}PCBM, and C_{70}PCBM. The gray, white, and red atoms represent carbon, hydrogen, and oxygen, respectively.

screened range-separated functional by replacing the $1/r$ asymptotic behavior, which is correct in the gas phase, with the more general asymptotic $1/(\varepsilon r)$ evolution, which is required when the calculations are performed on the periodic crystal.[17] Phillips et al. used a range-separated functional with the same (IP-tuned) ω values for both the molecule and the crystal, but derived the solid-state IEs (EAs) by a PCM-ΔSCF correction based on the orbital energies of the isolated molecule.[8] However, since the range-separation parameter ω is typically considered to be a functional of the density,[39,66] it should not be expected that the tuned ω value found for the molecule is also "optimal" for the crystal, since the electron density will be influenced by polarization effects. While the present study builds on the insights gained from these previous works, its novelty comes from the fact that it connects the optimal tuning concept with the description of solid-state screening effects via a continuum polarization model. Since it does not require the implementation of a new functional and all calculations are carried out for the single molecule and not the periodic crystal, the proposed methodology is numerically very efficient and can be readily employed by DFT practitioners using most standard DFT codes.

In this context, it should also be noted that several investigations have examined the combination of optimally tuned range-separated hybrid functionals with continuum polarization models to simulate solvent effects, primarily in the context of calculating charge-transfer excitation energies using TD-DFT.[9,56,67] De Queiroz and Kümmel[68,69] have recently demonstrated that the combination of optimal-tuning techniques with solvation models such as PCM can, in fact, be problematic for such cases, as it generally leads to excitation energies that are too small for charge-transfer excitations. To circumvent these problems, these authors suggested taking the solvent molecules explicitly into account during the tuning process, which requires the use of a locally projected self-consistent field diagonalization technique. It is important to realize, however, two important differences between these investigations and ours. First, de Queiroz and Kümmel have studied solvated molecules, while we study (homogeneous) molecular crystals. Indeed, many of the problems with the IP tuning in solvent arise from the fact that the solvent molecules have a significantly different electronic structure than the solute molecules. As a consequence, the tuned functional can either describe the polarization of the solvent or the electronic structure of the solute correctly, but not both at the same level of accuracy. In our case, however, the nature of all molecules is the same. The second difference is that de Queiroz and Kümmel have studied optical excitation energies, while we are primarily interested in the frontier orbital energies, which are relevant for charge injection/transport. While the use of a PCM model can have a significant direct effect on the former, especially for charge-transfer excitations, it does not directly influence the latter.

Here, we investigate a series of eight representative organic semiconductors, namely pentacene, TIPS-pentacene, rubrene, 3,4,9,10-perylene tetracarboxylic dianhydride (PTCDA), the C_{60} and C_{70} fullerenes and their [6,6]-phenyl-butyric-acid-methyl-ester derivatives $PC_{60}BM$ and $PC_{70}BM$ (see Figure 1). While all these molecules have been studied previously using optimal tuning methods in the gas phase,[37,48,70] we here report the results obtained from the PCM tuning of their respective organic crystals. The basic idea is to employ the PCM model using the dielectric constant of the crystal to simulate the crystal environment during the IP-tuning process. We demonstrate that, in this way, the influence of the crystal environment can be reasonably well described without the need to explicitly account for the periodic crystal structure. As a consequence, quantitative descriptions of the IEs, EAs, and fundamental gaps (see Figure 2) are obtained, with an accuracy comparable to GW and in close agreement with solid-state experimental data.

2. COMPUTATIONAL METHODS

In range-separated functionals, short- and long-range exchange interactions are treated on a different footing by separating the Coulomb operator (r_{12}) into short-range and long-range contributions. Typically, this is achieved via the standard error function:

$$r_{12}^{-1} = r_{12}^{-1}\,\mathrm{erfc}(\omega r_{12}) + r_{12}^{-1}\,\mathrm{erf}(\omega r_{12})$$

DOI: 10.1021/acs.jctc.6b00225
J. Chem. Theory Comput. 2016, 12, 2906−2916

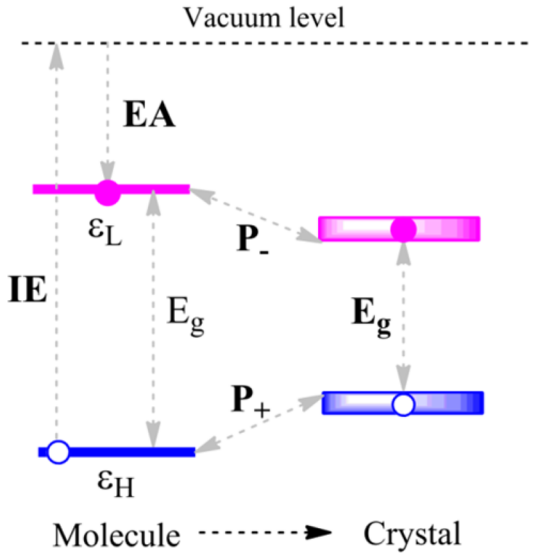

Figure 2. Schematic energy diagram of quasi-hole (electron) from gas-phase molecule to solid-state crystal. (Legend: IE, ionization energy; EA, electron affinity; ε_H, HOMO energy; ε_L, LUMO energy; E_g, transport gap; and P_+/P_-, polarization energy for hole/electron.

where the range-separation parameter ω quantifies the inverse of a distance at which the transition from short-range to long-range occurs. In long-range corrected hybrid functionals, short-range exchange interactions are treated via semilocal or global hybrid DFT, while the long-range exchange interactions are treated using full HF exchange. In the IP-tuning approach,[51] the range-separation parameter ω is determined nonempirically through minimizing $J(\omega) = |\varepsilon_H(N) + \mathrm{IP}(N)|$ for the neutral system, where $\mathrm{IP}(N)$ is derived from the total-energy difference between the neutral and cationic states. To allow for a better description of the HOMO−LUMO gap, an improved target functional has been suggested,[50]

$$J(\omega)^2 = \sum_{i=0}^{1} [\varepsilon_H(N+i) + \mathrm{IP}(N+i)]^2 \quad (1)$$

which simultaneously applies the above criterion for both neutral (N) and anion ($N+1$) systems. This gap-tuning procedure has been demonstrated to yield a good agreement between negative HOMO/LUMO energies and IE/EA values as follows:[37]

$$-\varepsilon_H(N) \cong \mathrm{IE}(N) \quad (2a)$$

$$-\varepsilon_L(N) \cong \mathrm{EA}(N) \quad (2b)$$

An important consequence of the tuning process is that the localization/delocalization error or many-electron self-interaction error is significantly reduced.[35,36]

All calculations were performed using the Gaussian 09 code.[71] To allow for a direct comparison with the GW calculations from refs 17, 18, and 23, the molecular geometries (see Figure 1) were optimized using the PBE functional[72] and 6-31G(d,p) basis set. The optimization of the range-separation parameter ω was performed based on the LC-ωPBE[46,73] functional and using the efficient "golden-ratio" algorithm, as described in our previous work[48,57] (see the Supporting Information for details). The IEs, EAs, and E_g values were then calculated using the optimally tuned LC-ωPBE functional (hereafter denoted as LC-ωPBE*) and the Truhlar "calendar" basis set may-cc-pVDZ.[74] The may-cc-pVDZ basis set is a simplified version of its augmented counterpart aug-cc-PVDZ, and is obtained by removing the two highest angular momentum diffuse functions for all of the atoms. This significantly reduces the computational cost without limiting the accuracy (see Table S1 in the Supporting Information). In addition to the PCM model, we also tested the conductor-like PCM (C-PCM) model in the case of pentacene and found hardly any differences between the optimal ω values and calculated orbital energies (see Table S2 in the Supporting Information). Therefore, the default PCM model was used throughout this work to simulate the polarization effects in the solid-state environment. All PCM parameters were chosen according to the default settings in Gaussian 09, except where explicitly stated otherwise.

Regarding the values of the dielectric constants to be used in PCM, we employed the static scalar dielectric constants as calculated by the random phase approximation (RPA) at the GW level, taken from the works of Kronik et al.[17,18] and Sai et al.[75] (see Table 1). Because of the absence of a GW value for TIPS-pentacene, we approximated the dielectric constant by using the same $\varepsilon = 3.6$ as for pentacene;[17] similarly, for $PC_{60}BM$, C_{70}, and $PC_{70}BM$, we used the same ε value (5.0) as for C_{60}.[17] Where available, we also provide the experimental ε values. As will be demonstrated below, the calculated optimal ω and, consequently, also the IEs are not very sensitive to the exact ε values (in the range of 3−5) considered for the organic crystals studied in this work.[5]

Table 1. Dielectric Constants (ε) and Optimal ω Values for the Molecular Systems Studied in This Work

	Isolated Molecule		Solid-State Environment		
			ε		
	ε	ω* (bohr^{-1})	scalar[a]	experimental[b]	ω* (bohr^{-1})
pentacene	1.0	0.187	3.6 (from ref 17)	4.0	0.046
TIPS−pentacene	1.0	0.144	3.6		0.041
rubrene	1.0	0.148	3.1 (from ref 75)		0.049
PTCDA	1.0	0.190	4.0 (from ref 18)	3.6	0.043
C60	1.0	0.183	5.0 (from ref 17)	4.1	0.031
C_{60}PCBM	1.0	0.174	5.0	3.9	0.031
C70	1.0	0.191	5.0		0.029
C_{70}PCBM	1.0	0.154	5.0		0.028

[a]The scalar dielectric constants were calculated at the GW/RPA level. [b]Experimental dielectric constants taken from Schwenn et al.[7]

DOI: 10.1021/acs.jctc.6b00225
J. Chem. Theory Comput. 2016, 12, 2906−2916

Table 2. Calculated $-\varepsilon_H$, $-\varepsilon_L$, and E_g of Various Molecules and Crystals[a]

	Quasiparticle Properties (eV)								
	LC-ωPBE*			GW			exp (UPS/IPES)		
system	$-\varepsilon_H$	$-\varepsilon_L$	E_g	$-\varepsilon_H$	$-\varepsilon_L$	E_g	IE	EA	E_g
Isolated Molecule									
pentacene	6.35	1.49	4.86	6.12	1.36	4.76[32 b]	6.59[70,76]	1.39[70,77]	5.20
						4.90[18 b]			
TIPS-pentacene	6.03	2.04	3.99			4.0[78]	6.28[12]		
rubrene	6.19	1.38	4.81	6.30	1.28	4.42[75]	6.41[79]	1.90[80]	4.5[80]
				6.22	0.96	5.26[36 c]			
PTCDA	8.14	3.07	5.07			5.10[18 b]	8.20[81]		
C_{60}	7.83	2.47	5.36	7.80	2.89	4.91[23 b]	7.69[70]	2.68[70]	5.01
				7.86	2.23	5.63[82 c]	7.59 ± 0.02[83]		
C_{60}PCBM	7.28	2.30	4.98	7.15	2.76	4.39[23]	7.17 ± 0.04[83]	2.63[84]	4.54
C_{70}	7.66	2.51	5.15	7.64	2.90	4.74[23]	7.47[23]	2.77[23]	4.70
				7.69	2.46	5.23[82 c]			
C_{70}PCBM	7.02	2.44	4.58						
MAD				0.09	0.30	0.28	0.17	0.28	0.38
Solid-State Environment									
pentacene	5.14	2.66	2.48	5.10	2.54	2.40[18 b]	4.90 ± 0.05	2.70 ± 0.03	2.20 ± 0.06[85]
						2.56[17]	5.05[14]		2.70[7]
TIPS-pentacene	5.11	2.99	2.12			2.10[78]	5.04[14]		
							5.84[12]		
rubrene	5.30	2.39	2.91			2.50[86]	5.30[79]	2.60[80]	2.70[80]
						2.80[75]			
PTCDA	6.62	3.92	2.70			2.70[18 b]	7.00[81]	3.90 ± 0.6[7]	2.5−2.8[18]
						3.00[10 b]			3.20 ± 0.4[87]
C_{60}	6.20	3.62	2.58	6.16	4.00	2.16[17]	6.17 ± 0.07[88]	4.50 ± 0.10[83]	2.5−2.6[89]
							6.45 ± 0.02[83]	3.50 ± 0.9[7]	
C_{60}PCBM	5.89	3.50	2.39				5.80 ± 0.15[90]	3.80 ± 0.45[90]	2.00
							5.96 ± 0.02[83]	3.90 ± 0.1[7]	2.06
C_{70}	6.13	3.63	2.50				6.02 ± 0.04[91]	4.10 ± 0.1[91]	1.90 ± 0.1
							6.35[92]	4.00 ± 0.04[92]	
C_{70}PCBM	5.84	3.50	2.34				5.90 ± 0.15[93]	3.70 ± 0.45[93]	2.20
							5.90[92]	3.81 ± 0.06[92]	2.09
MAD				0.04	0.25	0.13	0.12	0.29	0.25

[a]The GW and experimental values are listed for comparison when available from the literature. Numbers shown in superscripts are reference citations. [b]Self-consistent GW calculations or GW based on the HSE or PBE0 starting points. [c]From independent diffusion quantum Monte Carlo (QMC) calculations.

3. RESULTS AND DISCUSSION

Table 1 collects the optimally tuned ω values derived for the LC-ωPBE functional for the eight molecular systems in both the gas phase and the solid state, i.e., when using the PCM model with the respective dielectric constant of the molecular crystal during the tuning process. Compared to the default ω = 0.400 bohr^{-1} for LC-ωPBE, the optimal ω values significantly reduce to roughly 0.15−0.19 bohr^{-1} for gas-phase molecules. For the solid-state systems, which generally have small dielectric constants in the range of 3−5, the ω values decrease further to roughly 0.03−0.05 bohr^{-1}. As discussed in detail in refs 9 and 49, there is an inverse relationship between the tuned ω value and the spatial extension of the delocalization of electron density. Hence, the smaller ω values found for the simulated crystal environment are consistent with the expectation that the electron density is of a more delocalized nature in the crystal environment than for the individual molecules in the gas phase. As the range-separation parameter corresponds to an inverse distance, a decreased ω value indicates that the short-range DFT-GGA exchange will be replaced by long-range exact exchange (eX) at larger distance. In other words, there is less eX and more DFT-GGA exchange in the short- or medium-range exchange interactions. This also indicates that the reasonable description of molecular crystals requires the functionals to include less of the localized character arising from HF and more of the delocalized character coming from semilocal exchange.

To illustrate this behavior, Figure S1 in the Supporting Information shows the fraction of eX in various functionals versus the interelectronic distance r_{12}. In the following, we take the tuned ω value for pentacene as an example. At $r_{12} \approx 5.4$ atomic units (~2.8 Å, which corresponds roughly to twice the average distance of the C−C/C=C bonds or the width of a fused benzene ring), the tuned functional affords roughly 80% eX and 20% DFT-GGA exchange, while LC-ωPBE with a default ω of 0.4 bohr^{-1} gives almost 100% eX. However, when using the ω value found for the pentacene crystal, the tuned functional includes only roughly 25% eX and 75% DFT-GGA exchange at the r_{12} value of 5.4 atomic units. This finding indicates that, in order to accurately describe the polarization environment in the crystal, more DFT-GGA exchange and less eX are needed in the exchange functional. In this context, it is worth recalling the excellent prediction of the solid E_g value of

DOI: 10.1021/acs.jctc.6b00225
J. Chem. Theory Comput. 2016, 12, 2906−2916

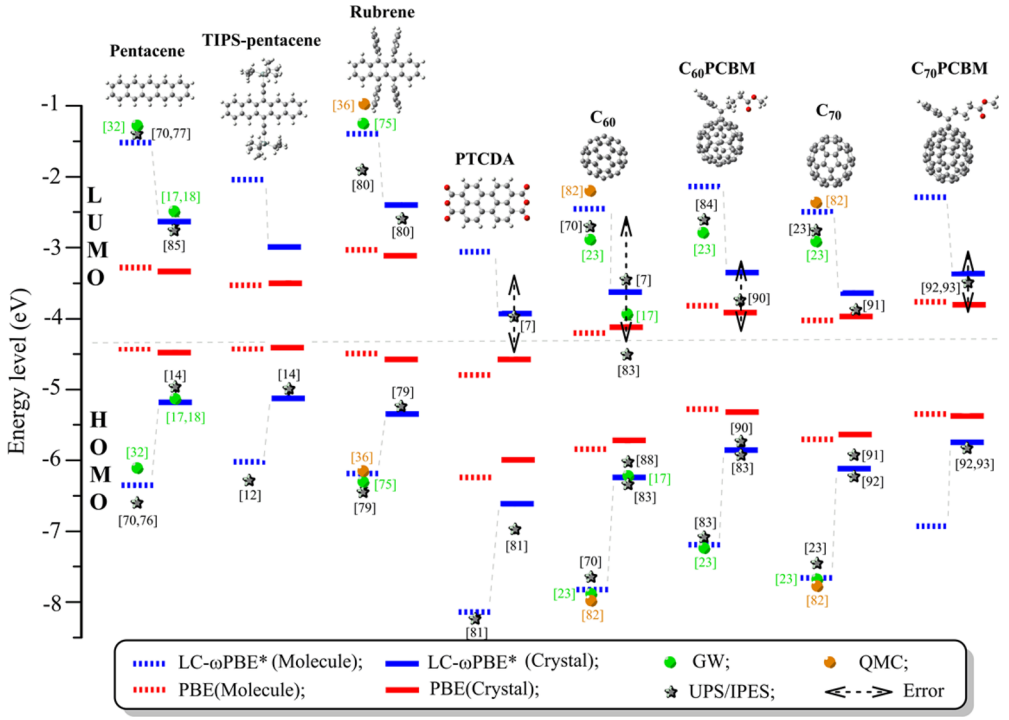

Figure 3. Calculated HOMO and LUMO energy levels from gas-phase molecules to solid-state crystals using the PBE (red) and LC-ωPBE* (blue) functionals; the benchmarks from (self-consistent) GW, quantum Monte Carlo (QMC), and experimental data are also presented, when available.

the pentacene crystal when using the PBE0 functional, which includes 25% of global eX.[17] A possible explanation for this "success" of PBE0 arises from the inverse dielectric constant of the pentacene crystal ($1/\varepsilon = 1/3.6 \approx 27\%$), which is indeed close to the 25% of eX included in PBE0. In this sense, the amount of HF exchange in PBE0 mimics the screening effects in the solid state. However, this adequacy does not translate to other molecular crystals such as solid benzene, whose dielectric constant is $\varepsilon = 2.3$ and, hence, requires less screening, i.e., a larger fraction of HF exchange.[17] At a much larger r_{12} value of ~22 atomic units (~12 Å, which is close to the length of a single pentacene molecule), there is still 20% DFT-GGA exchange in the tuned functional, indicating that the DFT-GGA exchange from the PCM-tuned functionals extends beyond a single molecule in the pentacene crystal.

Figure S2a in the Supporting Information shows how the tuned ω values are dependent on the dielectric constant ε used for the PCM during the tuning process. As the ε value increases, the ω value decreases exponentially. While the tuned ω changes rapidly with ε for small dielectric constants, the change when approaching common values for organic molecular crystals, that is, $\varepsilon = 3-5$, is almost negligible. For example, the tuned ω values for pentacene and TIPS-pentacene change only by 0.012 bohr^{-1} and 0.010 bohr^{-1}, respectively, when going from $\varepsilon = 3$ to $\varepsilon = 5$. Such a small decrease in ω typically results only in very small changes in IE, EA, and E_g.

Having established the procedure, we calculated the evolutions of the IEs, EAs, and E_g values in going from isolated molecules to solid-state environments. The results are compared to those obtained from PBE and GW calculations, as well as to experimental data in Table 2 and Table S5 in the Supporting Information. All the results are also graphically represented in Figure 3. For those molecules and crystals for which reliable benchmark data are available, we also provide the mean absolute deviation (MAD) of the IEs, EAs, and gaps.

For isolated molecules, the LC-ωPBE* functional yields ionization energies that are in excellent agreement with the GW IEs (MAD = 0.09 eV) and experimental IEs (MAD = 0.17 eV). The prediction of the electron affinities is not quite as accurate, but still shows acceptable MADs of 0.28 and 0.30 eV with respect to the GW and experimental values, respectively. It is interesting to note that the values found for the LUMOs of C_{60} and C_{70} agree well with the reliable independent-diffusion Quantum Monte Carlo (QMC) method, as shown in Table 2. Overall, also the calculated transport gaps predicted by the LC-ωPBE* functional agree reasonably well with the high-level GW (or QMC) results and experimental data, with MADs of 0.28 and 0.38 eV, respectively. As expected, the MADs for the PBE functional, with respect to the GW data (see Table S5 in the Supporting Information) are unacceptably large and calculated to be 1.54 eV for the IEs, 1.43 eV for the EAs, and 3.22 eV for the gaps.

For solid-state environments, there are two ways to simulate the polarization effects in molecular crystals: (i) to perform the tuning in the gas phase and then calculate the frontier orbital energies using the PCM model; or (ii) to perform both the tuning and the calculation of the frontier orbital energies using PCM. As shown in Table S4 in the Supporting Information, the simple addition of the PCM model to the gas-phase tuned functional completely fails to describe the polarization effects of crystals, resulting in HOMO and LUMO energy levels that barely change between the gas-phase and PCM calculations. This is not surprising, of course, since the PCM model only directly affects the total energy and not the eigenvalues, which are only indirectly affected via the SCF procedure. However, when the PCM tuning is performed, one obtains significantly smaller ω values, compared to tuning in the gas phase. As a result, good agreement of the calculated IE, EA, and E_g values of the organic crystals with MADs is found, with respect to the experimental data [GW data] of 0.12 [0.04] eV for the IEs, 0.29

DOI: 10.1021/acs.jctc.6b00225
J. Chem. Theory Comput. 2016, 12, 2906−2916

[0.25] eV for the EAs, and 0.25 [0.13] eV for the energy gaps. For a comparison, the MADs determined using the first method (gas-phase tuning + PCM) are significantly larger and calculated to be 1.45 [1.43] eV for the IEs, 1.47 [1.32] eV for the EAs, and 2.63 [2.38] eV for the transport gaps, as shown in Tables S4 and S5. The MADs obtained when using the PBE functional are calculated to be 0.57 [0.53] eV for the IEs, 0.37 [0.45] eV for the EAs, and 0.86 [1.12] eV for the gaps. Overall, these results indicate that the PCM-tuned LC-ωPBE* approach yields reliable IEs, EAs, and transport gaps for both single molecules in the gas phase and organic molecular crystals.

We now turn to a discussion of the evolution of the IE ($-\varepsilon_H$) values (calculated by combining optimal tuning and PCM), as a function of dielectric constant. As was already noted, the PCM-tuned LC-ωPBE* methodology can accurately reproduce the experimental IEs in the solid state within ~0.1 eV. When evaluating the IEs as a function of ε from 1.5 to 8.5, similar trends are observed in comparison to the case of optimal ω introduced above: The calculated IEs for pentacene and TIPS-pentacene only decrease by roughly 0.20 and 0.18 eV, respectively, when ε increases from 3 to 5 (see Figures S2b and S2c). This result is consistent with the fact that a larger polarizability of the solid-state environment leads to a more delocalized electronic structure and a decrease in IE.

Electronic polarization represents a critical parameter in organic semiconductor materials. In a polarizable environment, the energy to add or remove an electron from a given molecule decreases and the energy gap renormalizes (as illustrated in Figure 2). The GW approximation has been demonstrated to reliably capture the gap renormalization.[17] Hence, GW calculations allow the determination of the total solid-state polarization energy (P) from the change between the gas-phase gap and the solid-state gap. Here, we have calculated the solid-state polarization using the PCM-tuned LC-ωPBE* functionals; the results are summarized in Table 3. Since both the calculated

Table 3. Calculated Polarization Energies (P, eV) of Various Molecular Crystals Studied in This Work, with $P = E_g(\text{gas}) - E_g(\text{solid})$, as Illustrated in Figure 2

	Polarization Energy, P (eV)			
	PBE	LC-ωPBE*	GW	exp
pentacene	0.00	2.38	2.36	3.00
TIPS−pentacene	0.00	1.87	1.90	
rubrene	0.01	1.90	1.62	1.80
PTCDA	0.01	2.37	2.40	
C_{60}	0.00	2.78	2.75	2.41
C_{60}PCBM	0.01	2.59		2.54
C_{70}	0.01	2.65		2.80
C_{70}PCBM	0.01	2.24		

gas-phase and solid-state gaps are accurately predicted, also very accurate polarization energies are obtained. With respect to the experimental reference data, the accuracy is comparable to that obtained from GW. We note that, in contrast, semilocal exchange-correlation functionals such as PBE cannot describe the gap renormalization in going from gas phase to solid state.[17]

To further test whether our PCM-tuned approach indeed captures the polarization effect, we consider a classic electrostatic model of polarization associated with a charge in a dielectric.[17,18,87] In this simple model, the polarization energy is described as

$$P = \frac{e^2}{R}\left(1 - \frac{1}{\varepsilon}\right)$$

where e is the electron charge and R is an effective molecular radius that can be seen as a constant for a specific unit cell in the crystal. If the polarization effects are properly captured, the calculated value of P should be linear in $1 - (1/\varepsilon)$ for any ε. Figure 4 shows the P values computed as a function of $1 - (1/\varepsilon)$ for the pentacene and TIPS−pentacene crystals. The linear relation is indeed verified, which indicates that our approach successfully captures electrostatic polarization and confirms that our quantitative description of gap renormalization is not fortuitous. Interestingly, the plots in Figure 4 are also consistent with the effective molecular radius of TIPS−pentacene being somewhat larger than that of pentacene.

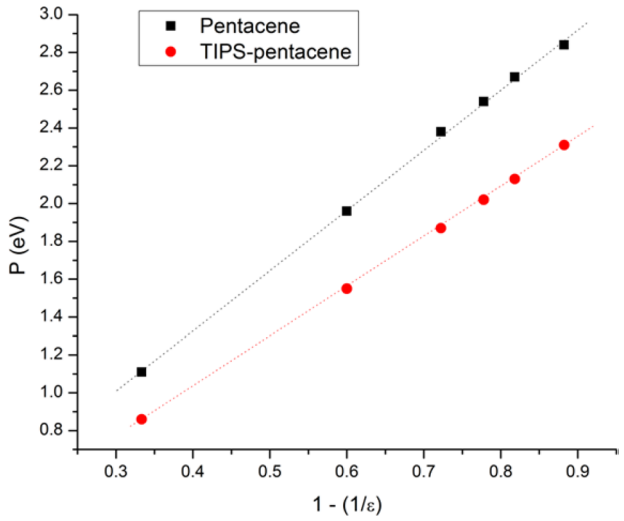

Figure 4. Calculated polarization energy P (eV) of pentacene and TIPS−pentacene crystals, as a function of $1 - (1/\varepsilon)$. Straight dashed lines are a linear fit.

At this stage, however, it is important to bear in mind the limitations of our model, which has been specifically designed to allow for a practical and numerically efficient estimation of the gas-to-crystal-phase shifts of quasiparticle energies in organic electronic materials. First, since the approach is based on calculations effectively involving a *single* molecule, it is unable to capture the effects associated with the details of the molecular packings in crystals or thin films, which determine the exact nature of the intermolecular interactions.[94] Because of the nature of the interactions of positively or negatively charged entities with their environment, the energetic stabilization of the positive and negative charges, i.e., the specific polarization energies for holes and electrons (P_+ and P_-) can be different. The optimal tuning plus PCM approach introduced here can quantitatively reproduce the gap renormalization and the total polarization energies ($P = P_+ + P_-$), but provides individual P_+ and P_- values that are very similar. This can be attributed to the fact that the PCM model employed here is an isotropic model in which the details of the molecular structures and packings are neglected. Therefore, our isotropic PCM-tuned methodology should not be used to distinguish between the individual polarization energies for holes and electrons; indeed, many factors that contribute to the descriptions of the P_+ and P_- energies[16,95] are not included in our model, such as the details

DOI: 10.1021/acs.jctc.6b00225
J. Chem. Theory Comput. 2016, 12, 2906−2916

of the electrostatic potentials and effects related to charge penetration, charge delocalization, and nuclear relaxation.

Second, by carrying out the IP tuning in the framework of the PCM instead of the explicit solid-state environment, the IPs in eq 1, which are calculated using energy differences between the neutral and charged systems, are in fact no longer the purely vertical IPs. Since the PCM takes into account the response of the dielectric medium to the presence of charges, the IPs calculated in this way are adiabatic with respect to the solid-state environment, yet still vertical with respect to the molecule itself. The IP theorem on which the tuning-procedure is based holds, however, only for purely vertical IPs. It can be expected that this inconsistency will introduce some error in the tuning procedure. However, since, for the reasons outlined above, application of the nonempirical tuning procedure to the full periodic crystal has not been achieved yet, we cannot currently provide an estimate for the size of this error. Given the accuracy of the PCM tuning results with respect to the theoretical and experimental reference data, however, it is expected that the error introduced by this approximation is either small or subject to a favorable cancellation of errors.

Finally, as noted above, the correct asymptotics of the exchange-correlation potential in the solid state is $1/(\varepsilon r)$, while here we employ the standard $1/r$ asymptotics, which is characteristic of standard long-range corrected functionals. The question of determining which of these two asymptotics would formally be the correct one in the context of PCM-tuning calculations, such as those carried out in this work, is, in fact, not straightforward to answer. On the one hand, it can be argued that all calculations are carried out on single molecules, so the $1/r$ asymptotics should be employed. On the other hand, the PCM model is supposed to model effects in the solid state, where the correct asymptotics would be $1/(\varepsilon r)$. Here, we have chosen to keep the standard $1/r$ asymptotics for the sake of practicality. The main goal of the approach proposed in the present work is to allow DFT practitioners to estimate the gas-to-solid-state shift using their electronic-structure code of choice; while standard long-range corrected functionals are implemented in most modern DFT codes, implementations of functionals with $1/(\varepsilon r)$ asymptotics are (still) rare. An alternative approach would be to (i) employ a long-range corrected functional with $1/(\varepsilon r)$ asymptotics and (ii) tune the range-separation parameter according to the PCM-tuning procedure. Since this procedure requires the implementation of a new functional and a large number of additional calculations, a detailed analysis of how it would compare to the procedure used here will be investigated in future work.

4. CONCLUSION AND OUTLOOK

We have presented a convenient, simple, and computationally inexpensive procedure that allows one to determine the ionization energies, electron affinities, transport gaps, and total polarization energies of organic molecular crystals or thin films with an accuracy comparable to GW calculations. This is achieved by combining the optimal tuning concept for range-separated hybrid functionals with a polarizable continuum model. The results on a series of eight molecular crystals/thin films were compared to GW reference calculations as well as experimental data, where available.

We attribute the success of the method to an appropriate balance between localization and delocalization effects included in the functionals for both isolated molecules and molecular crystals. The method requires the knowledge of the dielectric constant of the molecular crystal, which can be obtained from either higher-level calculations or the experiment. Once the dielectric constant is known, the gas-to-solid state energy shifts can be calculated from two single-point calculations based on a single molecule, with and without inclusion of the PCM model.

Given the accuracy of the method, its ease of application, and its numerical efficiency, we believe that it provides for an attractive alternative to GW calculations to estimate polarization effects. This opens the door to the study of systems that currently are beyond the reach of GW calculations.

■ ASSOCIATED CONTENT

Supporting Information

The Supporting Information is available free of charge on the ACS Publications website at DOI: 10.1021/acs.jctc.6b00225.

Computational details including the introduction of the tuning procedure described in this work and the effects of basis sets and polarizable models (PCM vs C-PCM); plot of the eX fraction, as a function of interelectronic distance; calculated $-\varepsilon_H$, $-\varepsilon_L$, and E_g of various molecules and crystals at the PBE/may-cc-pVDZ level; relationship of calculated IEs of pentacene/TIPS–pentacene, as a function of dielectric constant (PDF)

■ AUTHOR INFORMATION

Corresponding Authors

*E-mail: koerz@uni-potsdam.de (T. Körzdörfer).
*E-mail: jean-luc.bredas@kaust.edu.sa (J.-L. Brédas).

Notes

The authors declare no competing financial interest.

■ ACKNOWLEDGMENTS

The authors thank Prof. S. Kümmel for helpful discussions about the combination of the optimal tuning procedure with polarizable continuum solvation models. This work has been supported by King Abdullah University of Science and Technology (KAUST). We acknowledge the KAUST IT Research Computing Team for providing computational and storage resources.

■ REFERENCES

(1) Forrest, S. R.; Thompson, M. E. Introduction: Organic electronics and optoelectronics. *Chem. Rev.* **2007**, *107*, 923–925.
(2) Coropceanu, V.; Cornil, J.; da Silva Filho, D. A.; Olivier, Y.; Silbey, R.; Brédas, J.-L. Charge transport in organic semiconductors. *Chem. Rev.* **2007**, *107*, 926–952.
(3) Heeger, A. J. Semiconducting and Metallic Polymers: The Fourth Generation of Polymeric Materials (Nobel Lecture). *Angew. Chem., Int. Ed.* **2001**, *40*, 2591–2611.
(4) Brédas, J.-L.; Calbert, J. P.; da Silva Filho, D. A.; Cornil, J. Organic semiconductors: A theoretical characterization of the basic parameters governing charge transport. *Proc. Natl. Acad. Sci. U. S. A.* **2002**, *99*, 5804–5809.
(5) Brédas, J.-L. Mind the gap! *Mater. Horiz.* **2014**, *1*, 17–19.
(6) Kahn, A. Fermi level, work function and vacuum level. *Mater. Horiz.* **2016**, *3*, 7–10.
(7) Schwenn, P. E.; Burn, P. L.; Powell, B. J. Calculation of solid state molecular ionisation energies and electron affinities for organic semiconductors. *Org. Electron.* **2011**, *12*, 394–403.
(8) Phillips, H.; Zheng, Z.; Geva, E.; Dunietz, B. D. Orbital gap predictions for rational design of organic photovoltaic materials. *Org. Electron.* **2014**, *15*, 1509–1520.

DOI: 10.1021/acs.jctc.6b00225
J. Chem. Theory Comput. 2016, 12, 2906–2916

(9) Sun, H.; Autschbach, J. Electronic energy gaps for π-conjugated oligomers and polymers calculated with density functional theory. *J. Chem. Theory Comput.* **2014**, *10*, 1035−1047.
(10) Zade, S. S.; Bendikov, M. From oligomers to polymer: convergence in the HOMO−LUMO gaps of conjugated oligomers. *Org. Lett.* **2006**, *8*, 5243−5246.
(11) Krause, S.; Casu, M. B.; Schöll, A.; Umbach, E. Determination of transport levels of organic semiconductors by UPS and IPS. *New J. Phys.* **2008**, *10*, 085001.
(12) Griffith, O. L.; Anthony, J. E.; Jones, A. G.; Lichtenberger, D. L. Electronic properties of pentacene versus triisopropylsilylethynyl-substituted pentacene: environment-dependent effects of the silyl substituent. *J. Am. Chem. Soc.* **2010**, *132*, 580−586.
(13) Griffith, O. L.; Jones, A. G.; Anthony, J. E.; Lichtenberger, D. L. Intermolecular effects on the hole states of triisopropylsilylethynyl-substituted oligoacenes. *J. Phys. Chem. C* **2010**, *114*, 13838−13845.
(14) Qi, Y.; Mohapatra, S. K.; Bok Kim, S.; Barlow, S.; Marder, S. R.; Kahn, A. Solution doping of organic semiconductors using air-stable n-dopants. *Appl. Phys. Lett.* **2012**, *100*, 083305.
(15) Chan, C.; Kahn, A. N-doping of pentacene by decamethylcobaltocene. *Appl. Phys. A: Mater. Sci. Process.* **2009**, *95*, 7−13.
(16) Ryno, S. M.; Risko, C.; Brédas, J.-L. Impact of molecular packing on electronic polarization in organic crystals: the case of pentacene vs TIPS-pentacene. *J. Am. Chem. Soc.* **2014**, *136*, 6421−6427.
(17) Refaely-Abramson, S.; Sharifzadeh, S.; Jain, M.; Baer, R.; Neaton, J. B.; Kronik, L. Gap renormalization of molecular crystals from density-functional theory. *Phys. Rev. B: Condens. Matter Mater. Phys.* **2013**, *88*, 081204.
(18) Sharifzadeh, S.; Biller, A.; Kronik, L.; Neaton, J. B. Quasiparticle and optical spectroscopy of the organic semiconductors pentacene and PTCDA from first principles. *Phys. Rev. B: Condens. Matter Mater. Phys.* **2012**, *85*, 125307.
(19) Heimel, G.; Salzmann, I.; Duhm, S.; Koch, N. Design of organic semiconductors from molecular electrostatics. *Chem. Mater.* **2011**, *23*, 359−377.
(20) (a) Hedin, L. New Method for Calculating the One-Particle Green's Function with Application to the Electron-Gas Problem. *Phys. Rev.* **1965**, *139*, A796−A823. (b) Hybertsen, M. S.; Louie, S. G. Electron correlation in semiconductors and insulators: Band gaps and quasiparticle energies. *Phys. Rev. B: Condens. Matter Mater. Phys.* **1986**, *34*, 5390−5413.
(21) Aryasetiawan, F.; Gunnarsson, O. The GW method. *Rep. Prog. Phys.* **1998**, *61*, 237.
(22) Aulbur, W. G.; Jönsson, L.; Wilkins, J. W. Quasiparticle Calculations in Solids. In *Solid State Physics*; Henry, E., Frans, S., Eds.; Academic Press: New York, 1999; Vol. *54*, pp 1−218.
(23) Qian, X.; Umari, P.; Marzari, N. First-principles investigation of organic photovoltaic materials C_{60}, C_{70}, [C_{60}]PCBM, and bis-[C_{60}]PCBM using a many-body G_0W_0-Lanczos approach. *Phys. Rev. B: Condens. Matter Mater. Phys.* **2015**, *91*, 245105.
(24) Govoni, M.; Galli, G. Large scale GW calculations. *J. Chem. Theory Comput.* **2015**, *11*, 2680−2696.
(25) Rinke, P.; Qteish, A.; Neugebauer, J.; Freysoldt, C.; Scheffler, M. Combining GW calculations with exact-exchange density-functional theory: An analysis of valence-band photoemission for compound semiconductors. *New J. Phys.* **2005**, *7*, 126.
(26) Faber, C.; Attaccalite, C.; Olevano, V.; Runge, E.; Blase, X.; First-principles, G. W. calculations for DNA and RNA nucleobases. *Phys. Rev. B: Condens. Matter Mater. Phys.* **2011**, *83*, 115123.
(27) Marom, N.; Caruso, F.; Ren, X.; Hofmann, O. T.; Körzdörfer, T.; Chelikowsky, J. R.; Rubio, A.; Scheffler, M.; Rinke, P. Benchmark of GW methods for azabenzenes. *Phys. Rev. B: Condens. Matter Mater. Phys.* **2012**, *86*, 245127.
(28) Caruso, F.; Rinke, P.; Ren, X.; Scheffler, M.; Rubio, A. Unified description of ground and excited states of finite systems: The self-consistent GW approach. *Phys. Rev. B: Condens. Matter Mater. Phys.* **2012**, *86*, 081102.
(29) Körzdörfer, T.; Marom, N. Strategy for finding a reliable starting point for G_0W_0 demonstrated for molecules. *Phys. Rev. B: Condens. Matter Mater. Phys.* **2012**, *86*, 041110.
(30) Gallandi, L.; Körzdörfer, T. Long-range corrected DFT meets GW: vibrationally resolved photoelectron spectra from first principles. *J. Chem. Theory Comput.* **2015**, *11*, 5391−5400.
(31) Knight, J. W.; Wang, X.; Gallandi, L.; Dolgounitcheva, O.; Ren, X.; Ortiz, J. V.; Rinke, P.; Körzdörfer, T.; Marom, N. Accurate ionization potentials and electron affinities of acceptor molecules III: A benchmark of GW methods. *J. Chem. Theory Comput.* **2016**, *12*, 615−626.
(32) Blase, X.; Attaccalite, C.; Olevano, V. First-principles GW calculations for fullerenes, porphyrins, phtalocyanine, and other molecules of interest for organic photovoltaic applications. *Phys. Rev. B: Condens. Matter Mater. Phys.* **2011**, *83*, 115103.
(33) Bruneval, F.; Marques, M. A. L. Benchmarking the Starting Points of the GW Approximation for Molecules. *J. Chem. Theory Comput.* **2013**, *9*, 324−329.
(34) Gallandi, L.; Marom, N.; Rinke, P.; Körzdörfer, T. Accurate ionization potentials and electron affinities of acceptor molecules II: Non-empirically tuned long-range corrected hybrid functionals. *J. Chem. Theory Comput.* **2016**, *12*, 605−614.
(35) Körzdörfer, T.; Brédas, J.-L. Organic electronic materials: recent advances in the DFT description of the ground and excited states using tuned range-separated hybrid functionals. *Acc. Chem. Res.* **2014**, *47*, 3284−3291.
(36) Autschbach, J.; Srebro, M. Delocalization error and "functional tuning" in Kohn−Sham calculations of molecular properties. *Acc. Chem. Res.* **2014**, *47*, 2592−2602.
(37) Sun, H.; Autschbach, J. Influence of the delocalization error and applicability of optimal functional tuning in density functional calculations of nonlinear optical properties of organic donor-acceptor chromophores. *ChemPhysChem* **2013**, *14*, 2450−2461.
(38) Tozer, D. J. Relationship between long-range charge-transfer excitation energy error and integer discontinuity in Kohn−Sham theory. *J. Chem. Phys.* **2003**, *119*, 12697−12699.
(39) Kronik, L.; Stein, T.; Refaely-Abramson, S.; Baer, R. Excitation gaps of finite-sized systems from optimally tuned range-separated hybrid functionals. *J. Chem. Theory Comput.* **2012**, *8*, 1515−1531.
(40) Stein, T.; Autschbach, J.; Govind, N.; Kronik, L.; Baer, R. Curvature and frontier orbital energies in density functional theory. *J. Phys. Chem. Lett.* **2012**, *3*, 3740−3744.
(41) Ruzsinszky, A.; Perdew, J. P.; Csonka, G. I.; Vydrov, O. A.; Scuseria, G. E. Spurious fractional charge on dissociated atoms: Pervasive and resilient self-interaction error of common density functionals. *J. Chem. Phys.* **2006**, *125*, 194112.
(42) Mori-Sánchez, P.; Cohen, A. J.; Yang, W. Many-electron self-interaction error in approximate density functionals. *J. Chem. Phys.* **2006**, *125*, 201102.
(43) Perdew, J. P.; Zunger, A. Self-interaction correction to density-functional approximations for many-electron systems. *Phys. Rev. B: Condens. Matter Mater. Phys.* **1981**, *23*, 5048−5079.
(44) Yanai, T.; Tew, D. P.; Handy, N. C. A new hybrid exchange−correlation functional using the Coulomb-attenuating method (CAM-B3LYP). *Chem. Phys. Lett.* **2004**, *393*, 51−57.
(45) Savin, A.; Flad, H.-J. Density functionals for the Yukawa electron-electron interaction. *Int. J. Quantum Chem.* **1995**, *56*, 327−332.
(46) Vydrov, O. A.; Scuseria, G. E. Assessment of a long-range corrected hybrid functional. *J. Chem. Phys.* **2006**, *125*, 234109.
(47) Chai, J.-D.; Head-Gordon, M. Systematic optimization of long-range corrected hybrid density functionals. *J. Chem. Phys.* **2008**, *128*, 084106.
(48) Sun, H.; Zhong, C.; Brédas, J.-L. Reliable prediction with tuned range-separated functionals of the singlet−triplet gap in organic emitters for thermally activated delayed fluorescence. *J. Chem. Theory Comput.* **2015**, *11*, 3851−3858.
(49) Körzdörfer, T.; Sears, J. S.; Sutton, C.; Brédas, J.-L. Long-range corrected hybrid functionals for pi-conjugated systems: Dependence of

DOI: 10.1021/acs.jctc.6b00225
J. Chem. Theory Comput. 2016, 12, 2906−2916

the range-separation parameter on conjugation length. *J. Chem. Phys.* **2011**, *135*, 204107.
(50) Stein, T.; Kronik, L.; Baer, R. Reliable prediction of charge transfer excitations in molecular complexes using time-dependent density functional theory. *J. Am. Chem. Soc.* **2009**, *131*, 2818−2820.
(51) Stein, T.; Kronik, L.; Baer, R. Prediction of charge-transfer excitations in coumarin-based dyes using a range-separated functional tuned from first principles. *J. Chem. Phys.* **2009**, *131*, 244119.
(52) Refaely-Abramson, S.; Sharifzadeh, S.; Govind, N.; Autschbach, J.; Neaton, J. B.; Baer, R.; Kronik, L. Quasiparticle spectra from a nonempirical optimally tuned range-separated hybrid density functional. *Phys. Rev. Lett.* **2012**, *109*, 226405.
(53) Srebro, M.; Autschbach, J. Does a molecule-specific density functional give an accurate electron density? The challenging case of the CuCl electric field gradient. *J. Phys. Chem. Lett.* **2012**, *3*, 576−581.
(54) Sun, H.; Zhang, S.; Sun, Z. Applicability of optimal functional tuning in density functional calculations of ionization potentials and electron affinities of adenine-thymine nucleobase pairs and clusters. *Phys. Chem. Chem. Phys.* **2015**, *17*, 4337−4345.
(55) Tamblyn, I.; Refaely-Abramson, S.; Neaton, J. B.; Kronik, L. Simultaneous determination of structures, vibrations, and frontier orbital energies from a self-consistent range-separated hybrid functional. *J. Phys. Chem. Lett.* **2014**, *5*, 2734−2741.
(56) Moore, B.; Sun, H.; Govind, N.; Kowalski, K.; Autschbach, J. Charge-transfer versus charge-transfer-like excitations revisited. *J. Chem. Theory Comput.* **2015**, *11*, 3305−3320.
(57) Sun, H.; Zhang, S.; Zhong, C.; Sun, Z. Theoretical study of excited states of DNA base dimers and tetramers using optimally tuned range-separated density functional theory. *J. Comput. Chem.* **2016**, *37*, 684−693.
(58) Refaely-Abramson, S.; Jain, M.; Sharifzadeh, S.; Neaton, J. B.; Kronik, L. Solid-state optical absorption from optimally tuned time-dependent range-separated hybrid density functional theory. *Phys. Rev. B: Condens. Matter Mater. Phys.* **2015**, *92*, 081204.
(59) Foster, M. E.; Wong, B. M. Nonempirically tuned range-separated DFT accurately predicts both fundamental and excitation gaps in DNA and RNA nucleobases. *J. Chem. Theory Comput.* **2012**, *8*, 2682−2687.
(60) Mori-Sánchez, P.; Cohen, A. J.; Yang, W. Localization and delocalization errors in density functional theory and implications for band-gap prediction. *Phys. Rev. Lett.* **2008**, *100*, 146401.
(61) Vlček, V.; Eisenberg, H. R.; Steinle-Neumann, G.; Kronik, L.; Baer, R. Deviations from piecewise linearity in the solid-state limit with approximate density functionals. *J. Chem. Phys.* **2015**, *142*, 034107.
(62) Tomasi, J.; Mennucci, B.; Cammi, R. Quantum mechanical continuum solvation models. *Chem. Rev.* **2005**, *105*, 2999−3094.
(63) Mennucci, B. Polarizable continuum model. *Wiley Interdiscip. Rev.: Comput. Mol. Sci.* **2012**, *2*, 386−404.
(64) Lipparini, F.; Mennucci, B. Embedding effects on charge-transport parameters in molecular organic materials. *J. Chem. Phys.* **2007**, *127*, 144706.
(65) Skone, J. H.; Govoni, M.; Galli, G. Self-consistent hybrid functional for condensed systems. *Phys. Rev. B: Condens. Matter Mater. Phys.* **2014**, *89*, 195112.
(66) Baer, R.; Neuhauser, D. Density functional theory with correct long-range asymptotic behavior. *Phys. Rev. Lett.* **2005**, *94*, 043002.
(67) Autschbach, J. Charge-transfer excitations and time-dependent density functional theory: Problems and some proposed solutions. *ChemPhysChem* **2009**, *10*, 1757−1760.
(68) de Queiroz, T. B.; Kümmel, S. Tuned range separated hybrid functionals for solvated low bandgap oligomers. *J. Chem. Phys.* **2015**, *143*, 034101.
(69) de Queiroz, T. B.; Kümmel, S. Charge-transfer excitations in low-gap systems under the influence of solvation and conformational disorder: Exploring range-separation tuning. *J. Chem. Phys.* **2014**, *141*, 084303.
(70) Zhang, C.-R.; Sears, J. S.; Yang, B.; Aziz, S. G.; Coropceanu, V.; Brédas, J.-L. Theoretical study of the local and charge-transfer excitations in model complexes of pentacene-C_{60} using tuned range-separated hybrid functionals. *J. Chem. Theory Comput.* **2014**, *10*, 2379−2388.
(71) Frisch, M. J.; Trucks, G. W.; Schlegel, H. B.; Scuseria, G. E.; Robb, M. A.; Cheeseman, J. R.; Scalmani, G.; Barone, V.; Mennucci, B.; Petersson, G. A.; Nakatsuji, H.; Caricato, M.; Li, X.; Hratchian, H. P.; Izmaylov, A. F.; Bloino, J.; Zheng, G.; Sonnenberg, J. L.; Hada, M.; Ehara, M.; Toyota, K.; Fukuda, R.; Hasegawa, J.; Ishida, M.; Nakajima, T.; Honda, Y.; Kitao, O.; Nakai, H.; Vreven, T.; Montgomery, J. A.; Peralta, J. E.; Ogliaro, F.; Bearpark, M.; Heyd, J. J.; Brothers, E.; Kudin, K. N.; Staroverov, V. N.; Kobayashi, R.; Normand, J.; Raghavachari, K.; Rendell, A.; Burant, J. C.; Iyengar, S. S.; Tomasi, J.; Cossi, M.; Rega, N.; Millam, J. M.; Klene, M.; Knox, J. E.; Cross, J. B.; Bakken, V.; Adamo, C.; Jaramillo, J.; Gomperts, R.; Stratmann, R. E.; Yazyev, O.; Austin, A. J.; Cammi, R.; Pomelli, C.; Ochterski, J. W.; Martin, R. L.; Morokuma, K.; Zakrzewski, V. G.; Voth, G. A.; Salvador, P.; Dannenberg, J. J.; Dapprich, S.; Daniels, A. D.; Farkas, O.; Foresman, J. B.; Ortiz, J. V.; Cioslowski, J.; Fox, D. J. *Gaussian 09, Revision D.01*; Gaussian, Inc.: Wallingford, CT, 2009.
(72) Perdew, J. P.; Burke, K.; Ernzerhof, M. Generalized gradient approximation made simple. *Phys. Rev. Lett.* **1996**, *77*, 3865−3868.
(73) Vydrov, O. A.; Heyd, J.; Krukau, A.; Scuseria, G. E. Importance of short-range versus long-range Hartree-Fock exchange for the performance of hybrid density functionals. *J. Chem. Phys.* **2006**, *125*, 074106.
(74) Papajak, E.; Zheng, J.; Xu, X.; Leverentz, H. R.; Truhlar, D. G. Perspectives on basis sets beautiful: seasonal plantings of diffuse basis functions. *J. Chem. Theory Comput.* **2011**, *7*, 3027−3034.
(75) Sai, N.; Tiago, M. L.; Chelikowsky, J. R.; Reboredo, F. A. Optical spectra and exchange-correlation effects in molecular crystals. *Phys. Rev. B: Condens. Matter Mater. Phys.* **2008**, *77*, 161306.
(76) Gruhn, N. E.; da Silva Filho, D. A.; Bill, T. G.; Malagoli, M.; Coropceanu, V.; Kahn, A.; Brédas, J.-L. The vibrational reorganization energy in pentacene: molecular influences on charge transport. *J. Am. Chem. Soc.* **2002**, *124*, 7918−7919.
(77) Crocker, L.; Wang, T.; Kebarle, P. Electron affinities of some polycyclic aromatic hydrocarbons, obtained from electron-transfer equilibria. *J. Am. Chem. Soc.* **1993**, *115*, 7818−7822.
(78) Sharifzadeh, S.; Wong, C. Y.; Wu, H.; Cotts, B. L.; Kronik, L.; Ginsberg, N. S.; Neaton, J. B. Relating the physical structure and optoelectronic function of crystalline TIPS-pentacene. *Adv. Funct. Mater.* **2015**, *25*, 2038−2046.
(79) Sato, N.; Seki, K.; Inokuchi, H. Polarization energies of organic solids determined by ultraviolet photoelectron spectroscopy. *J. Chem. Soc., Faraday Trans. 2* **1981**, *77*, 1621−1633.
(80) Tomba, G.; Stengel, M.; Schneider, W.-D.; Baldereschi, A.; De Vita, A. Supramolecular self-assembly driven by electrostatic repulsion: The 1D aggregation of rubrene pentagons on Au(111). *ACS Nano* **2010**, *4*, 7545−7551.
(81) Dori, N.; Menon, M.; Kilian, L.; Sokolowski, M.; Kronik, L.; Umbach, E. Valence electronic structure of gas-phase 3,4,9,10-perylene tetracarboxylic acid dianhydride: Experiment and theory. *Phys. Rev. B: Condens. Matter Mater. Phys.* **2006**, *73*, 195208.
(82) Tiago, M. L.; Kent, P. R. C.; Hood, R. Q.; Reboredo, F. A. Neutral and charged excitations in carbon fullerenes from first-principles many-body theories. *J. Chem. Phys.* **2008**, *129*, 084311.
(83) Akaike, K.; Kanai, K.; Yoshida, H.; Tsutsumi, J. y.; Nishi, T.; Sato, N.; Ouchi, Y.; Seki, K. Ultraviolet photoelectron spectroscopy and inverse photoemission spectroscopy of [6,6]-phenyl-C61-butyric acid methyl ester in gas and solid phases. *J. Appl. Phys.* **2008**, *104*, 023710.
(84) Larson, B. W.; Whitaker, J. B.; Wang, X.-B.; Popov, A. A.; Rumbles, G.; Kopidakis, N.; Strauss, S. H.; Boltalina, O. V. Electron affinity of phenyl-C_{61}-butyric acid methyl ester (PCBM). *J. Phys. Chem. C* **2013**, *117*, 14958−14964.
(85) Koch, N.; Ghijsen, J.; Johnson, R. L.; Schwartz, J.; Pireaux, J. J.; Kahn, A. Physisorption-like interaction at the interfaces formed by pentacene and samarium. *J. Phys. Chem. B* **2002**, *106*, 4192−4196.

DOI: 10.1021/acs.jctc.6b00225
J. Chem. Theory Comput. 2016, 12, 2906−2916

(86) Berger, J. A.; Reining, L.; Sottile, F. Efficient GW calculations for SnO_2, ZnO, and rubrene: The effective-energy technique. *Phys. Rev. B: Condens. Matter Mater. Phys.* **2012**, *85*, 085126.
(87) Hill, I. G.; Kahn, A.; Soos, Z. G.; Pascal, R. A., Jr. Charge-separation energy in films of π-conjugated organic molecules. *Chem. Phys. Lett.* **2000**, *327*, 181−188.
(88) Sato, N.; Saito, Y.; Shinohara, H. Threshold ionization energy of C_{60} in the solid state. *Chem. Phys.* **1992**, *162*, 433−438.
(89) Takahashi, T.; Suzuki, S.; Morikawa, T.; Katayama-Yoshida, H.; Hasegawa, S.; Inokuchi, H.; Seki, K.; Kikuchi, K.; Suzuki, S.; Ikemoto, K.; Achiba, Y. Pseudo-gap at the Fermi level in K_3C_{60} observed by photoemission and inverse photoemission. *Phys. Rev. Lett.* **1992**, *68*, 1232−1235.
(90) Guan, Z.-L.; Kim, J. B.; Wang, H.; Jaye, C.; Fischer, D. A.; Loo, Y.-L.; Kahn, A. Direct determination of the electronic structure of the poly(3-hexylthiophene):phenyl-[6,6]-C_{61} butyric acid methyl ester blend. *Org. Electron.* **2010**, *11*, 1779−1785.
(91) Nogimura, A.; Akaike, K.; Nakanishi, R.; Eguchi, R.; Kanai, K. Electronic structure and surface morphology of [6,6]-phenyl-C_{71}-butyric acid methyl ester films. *Org. Electron.* **2013**, *14*, 3222−3227.
(92) Yoshida, H. Low-energy inverse photoemission study on the electron affinities of fullerene derivatives for organic photovoltaic cells. *J. Phys. Chem. C* **2014**, *118*, 24377−24382.
(93) Ratcliff, E. L.; Meyer, J.; Steirer, K. X.; Armstrong, N. R.; Olson, D.; Kahn, A. Energy level alignment in PCDTBT:PC_{70}BM solar cells: Solution processed NiOx for improved hole collection and efficiency. *Org. Electron.* **2012**, *13*, 744−749.
(94) Norton, J. E.; Brédas, J.-L. Polarization energies in oligoacene semiconductor crystals. *J. Am. Chem. Soc.* **2008**, *130*, 12377−12384.
(95) Ryno, S. M.; Lee, S. R.; Sears, J. S.; Risko, C.; Brédas, J.-L. Electronic polarization effects upon charge injection in oligoacene molecular crystals: description via a polarizable force field. *J. Phys. Chem. C* **2013**, *117*, 13853−13860.

DOI: 10.1021/acs.jctc.6b00225
J. Chem. Theory Comput. 2016, 12, 2906−2916